

Thermodynamical properties of graphene in noncommutative phase-space

Victor Santos^{a,b}, R. V. Maluf^a, C. A. S. Almeida^a

^a*Departamento de Física - Universidade Federal do Ceará (UFC) - C.P. 6030, 60455-760 Fortaleza-Ceará-Brazil*

^b*Institute for Gravitation and the Cosmos & Physics Department, Pennsylvania State University, University Park, PA 16801, U.S.A.*

Abstract

We investigated the thermodynamic properties of graphene in a noncommutative phase-space in the presence of a constant magnetic field. In particular, we determined the behaviour of the main thermodynamical functions: the Helmholtz free energy, the mean energy, the entropy and the specific heat. The high temperature limit is worked out and the thermodynamic quantities, such as mean energy and specific heat, exhibit the same features as the commutative case. Possible connections with the results already established in the literature are discussed briefly.

1. Introduction

Carbon, in its allotropic forms like graphite and diamond, takes up a prominent place in different branches of science. In particular, graphite can be thought as composed by stacking one-atom thick layers of carbon, called *graphene*. The physics of graphene has attracted attention from theoretical scientific community since experimental observations revealed the existence of electrical charge carriers that behave as massless Dirac quasi-particles [1, 2, 3, 4]. The reason for this is due to the unusual molecular structure of graphene. The Carbon atoms are arranged in a hexagonal lattice, similar to a honeycomb structure [5]. It was observed that the low-energy electronic excitations at the corners of graphene Brillouin zone can be described by a $2 + 1$ Dirac fermions with linear dispersion relation (massless) [3, 4]. This effect offers the prospect of testing several aspects of relativistic phenomena,

Email addresses: vsantos@gravity.psu.edu (Victor Santos), r.v.maluf@fisica.ufc.br (R. V. Maluf), carlos@fisica.ufc.br (C. A. S. Almeida)

which usually requires large energy, in experiments of the condensed matter physics such as chiral tunneling and Klein paradox [6, 7].

On the other side, the study of quantum systems in a noncommutative (NC) space has been the subject of much interest in last years, assuming that noncommutativity may be, in fact, a result of quantum gravity effects [8]. In these studies, some attention has been given to the models of noncommutative quantum mechanics (NCQM) [9]. The interest in this approach lies on the fact that NCQM is a fruitful theoretical laboratory where we can get some insight on the consequences of noncommutativity in field theory by using standard calculation techniques of quantum mechanics. In this context, several types of noncommutativity have been considered [10] and one case of particular importance is the so called noncommutative phase-space. This specific formulation is necessary to implement the Bose-Einstein statistics in the context of NCQM [11, 12].

The NC phase-space is based on the assumption that the spatial coordinates \hat{x}_i and the conjugate momenta \hat{p}_i are operators satisfy a deformed Heisenberg algebra, which in its simplest form can be described by the commutation relations:

$$[\hat{x}_i, \hat{x}_j] = i\theta_{ij}, \quad [\hat{p}_i, \hat{p}_j] = i\eta_{ij}, \quad [\hat{x}_i, \hat{p}_j] = i\hbar \left(\delta_{ij} + \frac{\theta_{ik}\eta_{jk}}{4\hbar^2} \right), \quad \text{with } i, j, k = 1, \dots, d, \quad (1)$$

where the deformation parameters $\theta_{ij} = \theta\epsilon_{ij}$ and $\eta_{ij} = \eta\epsilon_{ij}$ are real and antisymmetric constants matrices. These commutation relations can be explicitly implemented by means of coordinate transformations [13]:

$$\hat{x}_i = x_i - \frac{\theta_{ij}}{2\hbar} p_j, \quad \hat{p}_i = p_i + \frac{\eta_{ij}}{2\hbar} x_j, \quad (2)$$

where x_i and p_i are commutative variables that satisfy ordinary Heisenberg commutation relations,

$$[x_i, x_j] = 0, \quad [p_i, p_j] = 0, \quad [x_i, p_j] = i\hbar\delta_{ij}. \quad (3)$$

Recently, graphene in the framework of NCQM was studied by Bastos et al. [14], where the authors determined the Hamiltonian and the associated energy spectrum. It was shown that the electron states close to the Dirac points (K and K' points at the corners of graphene Brillouin zone) in a NC phase-space, subject to an external constant magnetic field, can be described by a massless $2D$ Dirac equation with only momenta noncommutativity. Otherwise, we would have a gauge symmetry breaking, which it is not observed in the graphene lattice [13].

These results, in association with suitable experimental data, may be used to investigate the role of noncommutativity in the graphene system and improve bounds on the magnitude of the corresponding noncommutative parameters. For instance, the issue concerning the thermodynamics properties of graphene modified by this kind of theory has not been addressed. Thus, using an approach similar to the cases of Dirac and Kemmer oscillators studied in Refs. [15, 16], we propose to evaluate the main thermodynamic functions that describe the thermal behaviour of this system in both cases; commutative and noncommutative. One such study with a focus on graphene is particularly interesting because this material has numerous applications for thermal industry, and it may be important in the understanding of heat conduction in low dimensions [17, 18, 19].

This work is outlined as follows. In Sec. 2, we summarize the key results of Ref. [14] which we will use in the sequel. In Sec. 3, the solution for the energy levels is utilized to calculate the partition function, and then all thermodynamic quantities that describe the thermal physics of NC graphene. The methodology used closely follows that developed in Refs. [15, 16]. Finally, in sec. 4, we present the conclusion and final remarks.

2. Graphene in a noncommutative phase-space

Before studying the thermal properties of graphene, let us first recall the fundamentals on the graphene physics in a NCQM approach. Here, we follow the steps described in Ref. [14]. The basic equation in the theory is the Dirac equation for a free massless particle:

$$i\hbar \frac{\partial \psi}{\partial t} = H_D \psi, \quad (4)$$

where H_D represents two copies of the massless Dirac-like Hamiltonian that describes the behaviour of electrons around each Dirac points K and K' , at the corners of Brillouin zone.

From this way, we can explicitly write:

$$H_D = \begin{pmatrix} H_K & 0 \\ 0 & H_{K'} \end{pmatrix} = v_F \begin{pmatrix} \boldsymbol{\sigma} \cdot \mathbf{p} & 0 \\ 0 & \boldsymbol{\sigma}^* \cdot \mathbf{p} \end{pmatrix}, \text{ and } \psi = \begin{pmatrix} \psi_K \exp(-\frac{i}{\hbar} E_K t) \\ \psi_{K'} \exp(-\frac{i}{\hbar} E_{K'} t) \end{pmatrix}, \quad (5)$$

such that $v_F \simeq 10^6 \text{m/s}$ is the Fermi velocity, $\mathbf{p} = -i\hbar(\partial_x, \partial_y, 0)$ is the two-dimensional momentum operator, $\boldsymbol{\sigma} = (\sigma_x, \sigma_y, \sigma_z)$ corresponds to the Pauli spin matrices and $\psi_{K(K')}$ are two-component wavefunction close to the K (K') point. Besides, $E_{K(K')} = \pm \hbar v_F |\mathbf{k}|$ represents the eigenvalues associated with the positive/negative energy band.

Considering an external homogeneous magnetic field, $\mathbf{B} = B_0 \hat{z}$, we must make the usual minimal substitution $\mathbf{p} \rightarrow \mathbf{p} - e\mathbf{A}$ in the free Hamiltonian (5), such that

$$H_K = v_F \sigma_i (p_i + \frac{eB_0}{2} \epsilon_{ij} x_j), \quad i, j = 1, 2, \quad (6)$$

where the vector potential is written in the symmetric gauge $\mathbf{A} = \frac{B_0}{2}(-y, x, 0)$. A similar equation can also be obtained for the Dirac point K' .

We can diagonalize the Hamiltonian (6) with an appropriate set of annihilation and creation operators, and obtain the following expression for the energy eigenvalues [14]

$$E_K = \pm \frac{\sqrt{2}\hbar v_F}{l_B} \sqrt{n}, \quad n = 0, 1, 2, \dots, \quad (7)$$

where $l_B = \sqrt{\hbar/eB_0}$ is called magnetic length.

On NC phase-space the Dirac Hamiltonian of graphene can be achieved through the shift given in Eq. (2). However, in order to preserve the gauge invariance on the graphene sheet, it should be required that the noncommutativity is nonzero only in momentum coordinates [13]. Thus, the Eq. (6) becomes

$$H_K^{\text{NC}} = v_F \sigma_i (p_i + \frac{eB_0}{2} \mu \epsilon_{ij} x_j), \quad i, j = 1, 2, \quad (8)$$

where

$$\mu = \left(1 + \frac{\eta}{eB_0 \hbar}\right). \quad (9)$$

Finally, it is possible to show that the energy spectrum takes the following form

$$E_K = \pm \frac{\sqrt{2}\hbar v_F}{l_B} \sqrt{(1 + \bar{\eta})n}, \quad n = 0, 1, 2, \dots, \quad (10)$$

with $\bar{\eta}$ being a dimensionless constant related to the noncommutative parameter η by means of $\bar{\eta} = (l_B^2/\hbar^2)\eta$.

3. Thermal properties of graphene in a noncommutative phase-space

3.1. Theoretical framework

In working out the thermal properties of graphene system, let us begin by defining the fundamental object in statistical mechanics, the canonical

partition function Z . Given the energy spectrum of graphene, we can define the partition function by a sum over all states s of the system, via

$$Z = \sum_s \exp(-\beta E_s), \quad \beta = \frac{1}{k_B T}, \quad (11)$$

where k_B is the Boltzmann constant and T is the equilibrium temperature.

The entire thermodynamics of NC graphene can be derived from the partition function Z and the Eq. (10). The most important thermodynamic functions for our analysis are the Helmholtz free energy F , the mean energy U , the entropy S and the specific heat C , defined by the following expressions:

$$F = -\frac{1}{\beta} \ln Z, \quad (12)$$

$$U = -\frac{\partial}{\partial \beta} \ln Z, \quad (13)$$

$$S = k_B \beta^2 \frac{\partial F}{\partial \beta}, \quad (14)$$

$$C = -k_B \beta^2 \frac{\partial U}{\partial \beta}. \quad (15)$$

We are now in condition to perform the numerical calculations of the partition function and all other thermodynamics quantities. To this end, it is convenient to introduce the dimensionless variables,

$$\bar{\beta} = \frac{1}{\tau}, \quad \tau = \frac{l_B}{\sqrt{2\hbar} v_F} \frac{1}{\beta}, \quad (16)$$

and rewrite all the previous functions in terms of these new quantities. In this case, we get $F \rightarrow \bar{F} = \frac{l_B}{\sqrt{2\hbar} v_F} F = -\frac{1}{\bar{\beta}} \log Z$, $U \rightarrow \bar{U} = \frac{l_B}{\sqrt{2\hbar} v_F} U = -\frac{\partial}{\partial \bar{\beta}} \log Z$, $S \rightarrow \bar{S} = \frac{S}{k_B} = \bar{\beta}^2 \frac{\partial \bar{F}}{\partial \bar{\beta}}$ and $C \rightarrow \bar{C} = \frac{C}{k_B} = -\bar{\beta}^2 \frac{\partial \bar{U}}{\partial \bar{\beta}}$, which are now all dimensionless functions. The remainder of the calculation procedure follows in a similar fashion to that described in Refs. [15, 16].

Using the Eq. (10), the partition function reads

$$Z = 1 + \sum_{n=0}^{\infty} e^{-\bar{\beta} \sqrt{an+a}}, \quad (17)$$

with $a = 1 + \bar{\eta}$. Let us note that the definition for the parameter a encompasses the noncommutative as well as the commutative case ($\bar{\eta} = 0$). The integral test ensures the convergence of the series, since the integral

$$\int_0^{\infty} dx e^{-\bar{\beta} \sqrt{ax+a}} = \frac{2}{a \bar{\beta}^2} e^{-\bar{\beta} \sqrt{a}} (1 + \bar{\beta} \sqrt{a}), \quad (18)$$

is finite. To evaluate the sum in (17) and determine the high temperature limit, we will employ the Euler-Mclaurin summation formula given by

$$\begin{aligned} \sum_{n=a}^b f(n) &= \int_a^b dt f(t) + \frac{1}{2}[f(b) + f(a)] + \sum_{i=2}^k \frac{b_i}{i!} [f^{(i-1)}(b) - f^{(i-1)}(a)] \\ &\quad - \int_a^b dt \frac{B_k(\{1-t\})}{k!} f^{(k)}(t), \end{aligned} \quad (19)$$

where a and b are arbitrary real numbers with difference $b-a$ being a positive integer number. B_k and b_n are Bernoulli polynomials and Bernoulli numbers, respectively, and k is any positive integer. The symbol $\{x\}$ for a real number x denotes the fractional part of x [20].

According to the relations (17) and (19), and considering $f(n) = \exp[-\bar{\beta}\sqrt{an+a}]$, the partition function Z can explicitly be written as

$$Z = 1 + \frac{1}{2}e^{-\bar{\beta}\sqrt{a}} + \frac{2}{a\bar{\beta}^2}e^{-\bar{\beta}\sqrt{a}}\left(1 + \bar{\beta}\sqrt{a}\right) - \sum_{i=2}^k \frac{b_i}{i!} f^{(i-1)}(0) + R_k, \quad (20)$$

with

$$R_k = \int_0^\infty dt \frac{B_k(\{1-t\})}{k!} f^{(k)}(t), \quad (21)$$

being the remainder term. The accuracy of approximation in (20) depends on the asymptotic behaviour of the remainder term R_k while k goes to infinity. In order to get a glimpse of the convergence speed, we display the behaviour of R_k in Figures 1 and 2, where the number of terms is $k \leq 25$. Let us note that the remainder term quickly decreases, becoming of the order of 10^{-5} after the summation of 10 terms of the series, and hence, for our purpose it is sufficient to take the summation of $k = 50$ in Euler-Maclaurin expansion for the partition function.

Before discussing the main results, we consider what happens in the higher temperatures limit to the case of the mean energy U and the specific heat C . In this regime, the dimensionless parameter $\bar{\beta}$ is very small and we can approximate the partition function by

$$Z \simeq \frac{2}{a\bar{\beta}^2}, \quad (22)$$

which leads to the following asymptotic limits

$$\bar{U} \simeq \frac{2}{\bar{\beta}}, \quad (23)$$

$$\bar{C} \simeq 2, \quad (24)$$

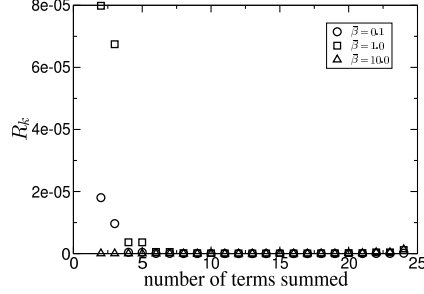


Figure 1: Plots of the remainder term R_k for the commutative case $\bar{\eta} = 0$.

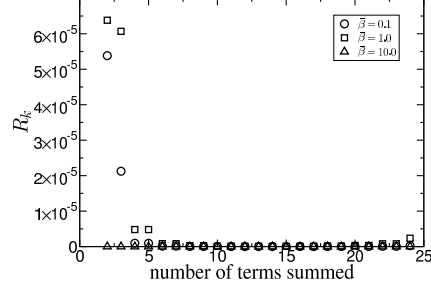


Figure 2: Plots of the remainder term R_k for the NC case with $\bar{\eta} = 0.1$.

where the bar denotes dimensionless quantities. We note that the dependence on the noncommutative parameter $\bar{\eta}$ is removed. Besides, these limits follow the Dulong-Petit law for an ultra-relativistic ideal gas. In such case, the average energy and specific heat are twice that of the non-relativistic limit. It is worth mentioning that similar results were observed for the Dirac and Kemmer oscillators in a thermal bath [15, 16].

3.2. Results and discussions

We are now ready to present our calculations for the thermodynamic properties of graphene, in a NC phase-space. All quantities were computed as a function of the dimensionless temperature τ , defined by $\tau = (l_B/\sqrt{2}\hbar v_F)k_B T$. The only free parameter that remains to be fixed is $\bar{\eta}$, and it is linked to the momentum noncommutative parameter η by the relation $\bar{\eta} = (l_B^2/\hbar^2)\eta$. Several bounds for the magnitude of this η -parameter have been determined in the literature. For example, in Ref. [13] a stringent bound on η , namely, $\sqrt{\eta} \lesssim 2.26 \times 10^{-6} \text{eV}/c$ was obtained, with the analysis of the hyperfine structure of hydrogen. Concerning the graphene system in the presence of a magnetic field, infrared spectroscopy experiments can be used to establish an upper bound of $\bar{\eta} < 0.069$, which implies that the magnitude of the parameter η not be larger than $\sqrt{\eta} < 8.6 \text{eV}/c$ [14]. This result is less restrictive than the early bound, however, it is more consistent with typical energy scales and experimental setups of graphene. Thereby, in the present approach, we will assume that the noncommutative effects are relevant at the interval $0 < \bar{\eta} < 0.1$. In order to illustrate the behavior of the

thermodynamic functions with respect to the parameter $\bar{\eta}$, let us consider the four different values $\bar{\eta} = 0.00$ (commutative case), 0.01, 0.04 and 0.07.

As a general result, we observed that the noncommutativity effects are very small and in the limit $\bar{\eta} \rightarrow 0$ all curves agree with the commutative case. The Helmholtz free energy \bar{F} for the commutative (solid line) and noncommutative (dashed lines) systems are shown in Figure 3. In any case it decreases with temperature, as expected. One observes that the free energies coincide at low temperatures, but occurs a **tiny** separation that increases with temperature and with the magnitude of the noncommutative parameter $\bar{\eta}$. From Figure 4, we can observe the behaviour of the mean energy with temperature. The plots of the mean energy, for different values of $\bar{\eta}$, do not differ significantly, and at the asymptotic limit, all the curves behave as linear functions of temperature. This is an expected result in view of our previous discussion.

Figure 5 provides the entropy curves of graphene for some values of $\bar{\eta}$. As in the case of the free energy, the behaviour of the entropy for commutative and noncommutative cases is similar at low temperatures. Note that the separation of the curves increases when the parameter $\bar{\eta}$ grows. Here, the effect of noncommutativity is to deviate to a lower value the entropy, in contrast to the free energy. Indeed, note that the curves with $\bar{\eta} \neq 0$ are located below the solid curve which represents the commutative case. This effect is expected because it is known that the noncommutativity leads to a decrease of the degeneracy in physical systems, reflecting a reduction of the entropy in a NC phase-space [21, 22].

Finally, let us analyze the behaviour of the specific heat as shown in Figure 6. Our calculations reveal that the noncommutative profiles change in the intermediate temperature range (about $\tau = 0.95$, approximately). We note that for low τ values the dashed lines are located below the solid line while the opposite occurs for large τ values (see insertion with broadened plots in Fig. 6). In particular, at high temperature regime all curves coincide with the limit value obtained in Eq. (24).

4. Conclusion

In the present work, we have studied the thermodynamic properties of graphene in a NC phase-space with the presence of an external constant magnetic field. Here, starting from the well-known Dirac Hamiltonian and its noncommutative extension presented in Ref. [14], we used the solutions of the energy spectrum in the numerical evaluation of the canonical partition function.

In the sequel, we have determined the main thermodynamic functions in both cases, commutative and noncommutative. The results are depicted in Figures 3, 4, 5 and 6. The overall behaviour of the thermodynamic functions indicates that the noncommutativity produces a small deviation around the usual commutative profile, and this deviation is positive for the free energy and negative for the entropy. Moreover, the curves for the mean energy and the specific heat are in agreement with the asymptotic values as given in Eqs. (22) and (24), respectively.

Finally, we expect in the near future, once obtained experimental measurements of high accuracy involving the thermodynamical properties of graphene, our results may be used as a good tool to study these properties. Also, we intend to investigate the possibility of new features of graphene can be described by NC models.

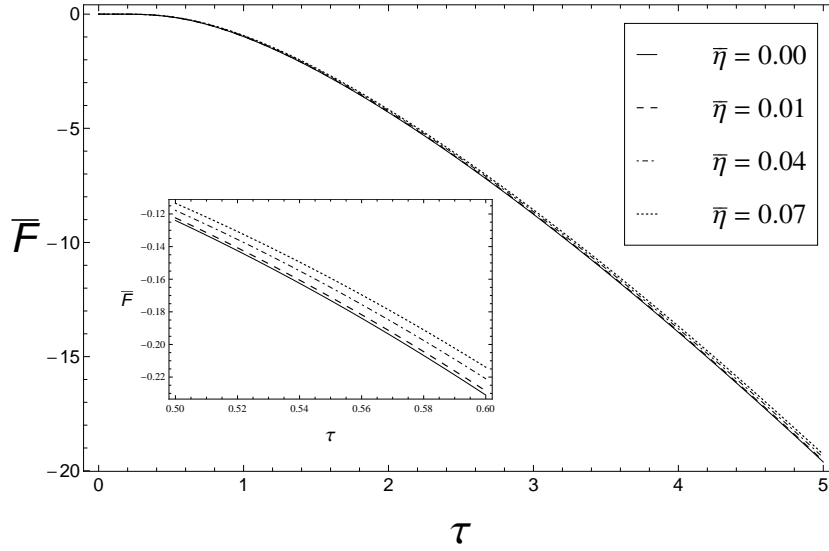


Figure 3: The free energy for the Dirac particle as a function of the dimensionless temperature τ , for different values of the noncommutativity parameter $\bar{\eta}$.

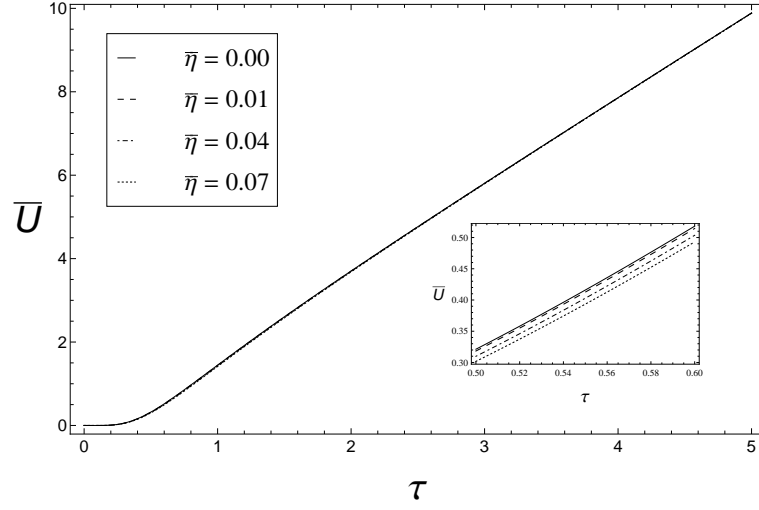


Figure 4: The mean energy as a function of the dimensionless temperature τ , for different values of the noncommutativity parameter $\bar{\eta}$.

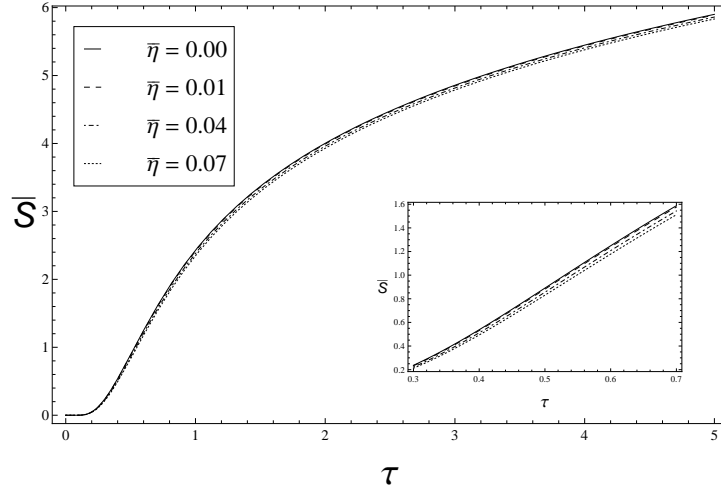


Figure 5: The entropy as a function of the dimensionless temperature τ , for different values of the noncommutativity parameter $\bar{\eta}$.

Acknowledgments

The authors thank the Coordenação de Aperfeiçoamento de Pessoal de Nível Superior (CAPES), and the Conselho Nacional de Desenvolvimento

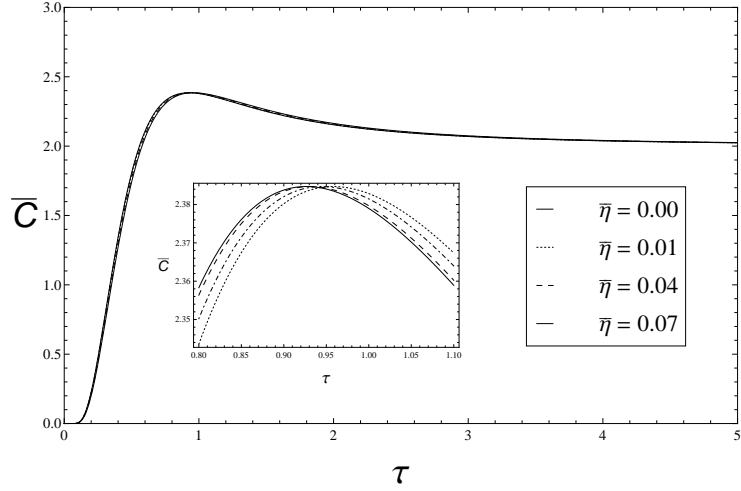


Figure 6: The specific heat as a function of the dimensionless temperature τ , for different values of the noncommutativity parameter $\bar{\eta}$.

Científico e Tecnológico (CNPq) for financial support.

References

- [1] K. S. Novoselov et al., Science **306**, 666 (2004).
- [2] K. S. Novoselov et al., Proc. Natl. Acad. Sci. **102**, 10451 (2005).
- [3] A. H. Castro Neto, F. Guinea, N. M. R. Peres, K. S. Novoselov and A. K. Geim, Rev. Mod. Phys. **81**, 109 (2009).
- [4] N. Peres, Rev. Mod. Phys. **82**, 2673 (2010).
- [5] Charles L. Fefferman and Michael I. Weinstein, J. Amer. Math. Soc. **25**, 1169 (2012).
- [6] M. I. Katsnelson, K. S. Novoselov, and A. K. Geim, Nat. Phys. **2**, 620 (2006).
- [7] M. I. Katsnelson, Mater. Today **10**, 20 (2007b).
- [8] C. Duval, P. A. Horvathy, Phys. Lett. B **479**, 284 (2000); V. P. Nair and A. P. Polychronakos, Phys. Lett. B **505**, 267 (2001); S. Bellucci,

- A. Nersessian and C. Sochichiu, Phys. Lett. B **522**, 345 (2001); R. Banerjee, Mod. Phys. Lett. A **17**, 631 (2002); Ashok Das, H. Falomir, J. Gamboa and F. Mendez, Phys. Lett. B **670**, 407 (2009); P. Nicolini, Int. J. Mod. Phys. A **24**, 1229 (2009).
- [9] C. Duval, P. A. Horváthy, J. Phys. A: Math. Gen. **34**, 1 (2001); M. Gomes, V. G. Kupriyanov, and A. J. da Silva, Phys. Rev. D **81**, 085024 (2010); Roberto V. Maluf, Int. J. Mod. Phys. A **26**, 4991 (2011).
- [10] M. Gomes, V. G. Kupriyanov, Phys. Rev. D **79**, 125011 (2009); H. Falomir, J. Gamboa, J. Lopes-Sarrion, F. Mendez and P. A. G. Pisani, Phys. Lett. B **680**, 384 (2009).
- [11] V. P. Nair, A. P. Polychronakos, Phys. Lett B **505**, 267 (2001).
- [12] Jian-Zu Zhang, Phys. Lett. B **584**, 204 (2004).
- [13] O. Bertolami, R. Queiroz, Phys. Lett. A **375**, 4116 (2011).
- [14] C. Bastos, O. Bertolami, N. Dias, J. Prata, Int. J. Mod. Phys. A **28**, 1350064 (2013).
- [15] M. H. Pacheco, R. R. Landim, C. A. S. Almeida, Phys. Lett. A **311**, 93 (2003).
- [16] A. Boumali, Phys. Scr. **76**, 669 (2007).
- [17] A. A. Balandin, Nature materials, v. **10**, n. 8, 569 (2011).
- [18] E. Pop, V. Varshney, A. K. Roy, MRS Bull. **37**, 1273 (2012).
- [19] A. Alofi, G. P. Srivastava, Phys. Rev. B **87**, 115421 (2013).
- [20] M. Abramowitz, I. A. Stegun, *Handbook of Mathematical Functions with Formulas, Graphs, and Mathematical Tables*, 9th printing. New York: Dover, pp. 16 and 806, 1972.
- [21] B. Muthukumar, and P. Mitra, Phys. Rev. D **66**, 027701 (2002).
- [22] M. Najafizadeh, M. Saadat, Chinese Journal of Physics **51**, 94 (2013).